

## Search for the Flavor-Changing Neutral-Current Decays

$$D^+ \rightarrow \pi^+ \mu^+ \mu^- \text{ and } D^+ \rightarrow \pi^+ e^+ e^-$$

E. M. Aitala,<sup>8</sup> S. Amato,<sup>1</sup> J. C. Anjos,<sup>1</sup> J. A. Appel,<sup>5</sup> D. Ashery,<sup>14</sup> S. Banerjee,<sup>5</sup> I. Bediaga,<sup>1</sup> G. Blaylock,<sup>2</sup> S. B. Bracker,<sup>15</sup> P. R. Burchat,<sup>13</sup> R. A. Burnstein,<sup>6</sup> T. Carter,<sup>5</sup> H. S. Carvalho,<sup>1</sup> I. Costa,<sup>1</sup> L. M. Cremaldi,<sup>8</sup> C. Darling,<sup>18</sup> K. Denisenko,<sup>5</sup> A. Fernandez,<sup>11</sup> P. Gagnon,<sup>2</sup> S. Gerzon,<sup>14</sup> C. Gobel,<sup>1</sup> K. Gounder,<sup>8</sup> D. Granite,<sup>7</sup> A. M. Halling,<sup>5</sup> G. Herrera,<sup>4</sup> G. Hurvits,<sup>14</sup> C. James,<sup>5</sup> P. A. Kasper,<sup>6</sup> N. Kondakis,<sup>10</sup> S. Kwan,<sup>5</sup> D. C. Langs,<sup>10</sup> J. Leslie,<sup>2</sup> J. Lichtenstadt,<sup>14</sup> B. Lundberg,<sup>5</sup> A. Manacero,<sup>5</sup> S. MayTal-Beck,<sup>14</sup> B. Meadows,<sup>3</sup> J. R. T. de Mello Neto,<sup>1</sup> R. H. Milburn,<sup>16</sup> J. M. de Miranda,<sup>1</sup> A. Napier,<sup>16</sup> A. Nguyen,<sup>7</sup> A. B. d'Oliveira,<sup>3,11</sup> K. O'Shaughnessy,<sup>2</sup> K. C. Peng,<sup>6</sup> L. P. Perera,<sup>3</sup> M. V. Purohit,<sup>12</sup> B. Quinn,<sup>8</sup> S. Radeztsky,<sup>17</sup> A. Rafatian,<sup>8</sup> N. W. Reay,<sup>7</sup> J. J. Reidy,<sup>8</sup> A. C. dos Reis,<sup>1</sup> H. A. Rubin,<sup>6</sup> A. K. S. Santha,<sup>3</sup> A. F. S. Santoro,<sup>1</sup> A. J. Schwartz,<sup>10</sup> M. Sheaff,<sup>17</sup> R. A. Sidwell,<sup>7</sup> A. J. Slaughter,<sup>18</sup> J. G. Smith,<sup>7</sup> M. D. Sokoloff,<sup>3</sup> N. R. Stanton,<sup>7</sup> K. Sugano,<sup>2</sup> D. J. Summers,<sup>8</sup> S. Takach,<sup>18</sup> K. Thorne,<sup>5</sup> A. K. Tripathi,<sup>9</sup> S. Watanabe,<sup>17</sup> R. Weiss,<sup>14</sup> J. Wiener,<sup>10</sup> N. Witchey,<sup>7</sup> E. Wolin,<sup>18</sup> D. Yi,<sup>8</sup> R. Zaliznyak,<sup>13</sup> and C. Zhang<sup>7</sup>

(Fermilab E791 Collaboration)

<sup>1</sup>Centro Brasileiro de Pesquisas Físicas, Rio de Janeiro, Brazil

<sup>2</sup>University of California, Santa Cruz, California 95064

<sup>3</sup>University of Cincinnati, Cincinnati, Ohio 45221

<sup>4</sup>CINVESTAV, Mexico, Distrito Federal, Mexico

<sup>5</sup>Fermilab, Batavia, Illinois 60510

<sup>6</sup>Illinois Institute of Technology, Chicago, Illinois 60616

<sup>7</sup>Kansas State University, Manhattan, Kansas 66506

<sup>8</sup>University of Mississippi, University, Mississippi 38677

<sup>9</sup>The Ohio State University, Columbus, Ohio 43210

<sup>10</sup>Princeton University, Princeton, New Jersey 08544

<sup>11</sup>Universidad Autonoma de Puebla, Puebla, Mexico

<sup>12</sup>University of South Carolina, Columbia, South Carolina 29208

<sup>13</sup>Stanford University, Stanford, California 94305

<sup>14</sup>Tel Aviv University, Tel Aviv, Israel

<sup>15</sup>317 Belsize Drive, Toronto, Canada

<sup>16</sup>Tufts University, Medford, Massachusetts 02155

<sup>17</sup>University of Wisconsin, Madison, Wisconsin 53706

<sup>18</sup>Yale University, New Haven, Connecticut 06511

(Received 1 June 1995)

We report the results of a search for the flavor-changing neutral-current decays  $D^+ \rightarrow \pi^+ \mu^+ \mu^-$  and  $D^+ \rightarrow \pi^+ e^+ e^-$  in data from Fermilab charm hadroproduction experiment E791. No signal above background is found, and we obtain upper limits on branching fractions,  $B(D^+ \rightarrow \pi^+ \mu^+ \mu^-) < 1.8 \times 10^{-5}$  and  $B(D^+ \rightarrow \pi^+ e^+ e^-) < 6.6 \times 10^{-5}$ , at the 90% confidence level.

PACS numbers: 13.20.Fc, 11.30.Hv

Flavor-changing neutral-current (FCNC) decays have played a major role in our understanding of weak decays. For example, absence of an  $s \rightarrow d$  quark transition in neutral kaon decays led to the Glashow-Iliopoulos-Maiani mechanism [1] that predicted the charm quark. This Letter presents limits from Fermilab experiment E791 for FCNC decays of charm,  $D^+ \rightarrow \pi^+ \mu^+ \mu^-$ ,  $\pi^+ e^+ e^-$  [2], which would proceed through an effective  $c \rightarrow u$  quark transition. These decays are forbidden at tree level within the standard model, but can occur through higher-order loop diagrams and are thus sensitive to physics at very high mass scales [3].

Within the standard model, the contribution of short-distance electroweak processes to  $B(D^+ \rightarrow \pi^+ \ell^+ \ell^-)$  is expected to be less than  $10^{-8}$  [4]; in contrast, the best

published experimental limits are only  $(2-3) \times 10^{-3}$  ( $\pi^+ e^+ e^-$ ) [5] and  $2 \times 10^{-4}$  ( $\pi^+ \mu^+ \mu^-$ ) [6]. Three-body FCNC decays such as  $D^+ \rightarrow \pi^+ \ell^+ \ell^-$  are more sensitive to new physics involving vector or axial vector currents than are two-body decays such as  $D^0 \rightarrow \ell^+ \ell^-$ , because three-body decays do not suffer from helicity suppression imposed by angular momentum conservation.

Our search finds no evidence for FCNC  $D^+ \rightarrow \pi^+ \ell^+ \ell^-$  decays. We set branching-fraction limits that are an order of magnitude below those previously published.

Data were recorded from 500 GeV/c  $\pi^-$  interactions in five thin foils (one platinum, four diamond) separated by gaps of 1.34 to 1.39 cm. The E791 spectrometer is an upgrade of apparatus used in Fermilab charm

experiments E516, E691, and E769 [7]. Two dipole magnets bend particles in the horizontal plane for momentum analysis. Silicon microstrip detectors (6 in the beam, 17 downstream of the target) provide precision track and vertex reconstruction. A calorimeter [8] of lead and liquid scintillator, 19 m from the target, identifies electrons; scintillator strips 3.17 cm wide [9] are oriented transverse to the beam and alternate among three stereo projections. Muons are identified by a plane of 16 scintillation counters behind 15 interaction lengths of shielding, including the calorimeter. These counters, 24 m from the target, are each 14 cm high and 300 cm wide, and measure displacement in the nonbend plane. Information from two segmented Čerenkov counters is not used in this analysis.

E791 recorded  $2 \times 10^{10}$  events with a loose transverse energy trigger. After reconstruction, events with evidence of multiple vertices were kept for further analysis.

To search for  $D^+$  FCNC decays in an unbiased way, track and vertex selection criteria for all  $D^+$  decays were determined from the Cabibbo-suppressed mode  $D^+ \rightarrow \pi^- \pi^+ \pi^+$ . These criteria, also nearly optimal for FCNC modes, maximize  $N_S/\sqrt{N_B}$ , where  $N_S$  and  $N_B$  are the respective numbers of signal and background events for  $D^+ \rightarrow \pi^- \pi^+ \pi^+$ . We obtain  $N_S = 1057$ ,  $N_B = 920$  events. Good mass resolution cleanly separates this signal from  $D^+ \rightarrow K^- \pi^+ \pi^+$  feedthrough without Čerenkov information or antiselection of the  $D^+ \rightarrow K^- \pi^+ \pi^+$  peak.

We require a three-prong secondary vertex to be separated by  $>20\sigma_L$  from the primary vertex and by  $>5.0\sigma_L$  from the closest material in the target foils, where  $\sigma_L$  in each case is the calculated longitudinal resolution in the measured separation. The summed momentum vector of the three tracks from this secondary vertex must miss the primary vertex by  $<40 \mu\text{m}$  in the plane perpendicular to the beam. We form the ratio of each track's smallest distance from the secondary vertex to that from the primary vertex, and require the product of these ratios to be  $<0.001$ . Finally, the net momentum of the  $D^+$  candidate transverse to the line connecting the primary and secondary vertices must be  $<250 \text{ MeV}/c$ .

The mean momentum of surviving  $D^+$  mesons is  $80 \text{ GeV}/c$ . Longitudinal and transverse position resolutions for the primary vertex are  $350$  and  $6 \mu\text{m}$ , respectively. For secondary vertices from  $D^+$  decays, the transverse resolution is about  $9 \mu\text{m}$ , nearly independent of momentum; the longitudinal resolution is  $390 \mu\text{m}$  at  $80 \text{ GeV}/c$  and increases by  $30 \mu\text{m}$  every  $10 \text{ GeV}/c$ .

The  $K^- \pi^+ \pi^+$  signal (Fig. 1) obtained with the above selection criteria serves as normalization for the FCNC branching fractions. A fit by a Gaussian signal and an exponential background gives  $37000 D^+ \rightarrow K^- \pi^+ \pi^+$  events and a  $D^+$  mass resolution of  $12.6 \pm 0.1 \text{ MeV}/c^2$ .

In addition to meeting the above selection criteria, candidates for  $D^+ \rightarrow \pi^+ \mu^+ \mu^-$  must have two oppositely charged tracks from the candidate decay vertex identified as muons. Muon counter efficiencies were measured to

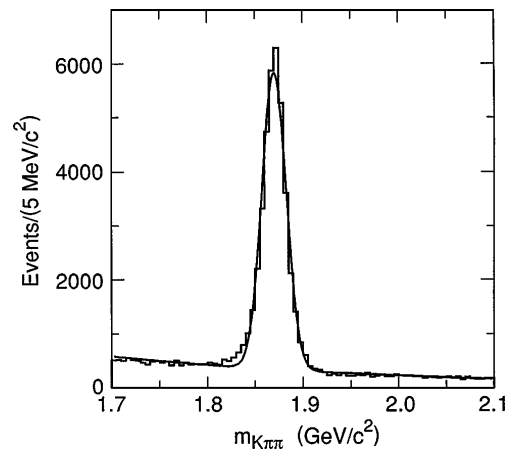


FIG. 1. Mass spectrum of candidate  $D^+ \rightarrow K^- \pi^+ \pi^+$  events with final optimized selection criteria, used to provide the normalizing signal for FCNC analyses. The curve is a fit to a Gaussian signal and an exponential background.

be  $(99 \pm 1)\%$  in special runs using independent muon identification (ID). False muon ID in E791 has two major sources: pion and kaon decay in flight, and misassociation with a counter fired by another track in the event. Because directions and momenta of charged particles are measured in tracking devices upstream of thick absorbing material in the muon system, predicted positions at the scintillation counters of low-momentum particles are smeared by multiple scattering. We require a signal from a muon counter whose closest edge is within  $N_\sigma \sigma_{MS}$  of the track's projected vertical position, where  $\sigma_{MS}$  is the predicted root-mean-square position error due to multiple scattering for a muon of the measured momentum. Final values of  $N_\sigma$  (1.0) and minimum momentum  $p_{\min}$  ( $7 \text{ GeV}/c$ ) were chosen in an unbiased way by optimizing  $S_{MC}/\sqrt{B_{\text{data}}}$ , where  $S_{MC}$  is a Monte Carlo FCNC signal and  $B_{\text{data}}$  is the background of misidentified hadrons in data outside the FCNC signal region. For  $N_\sigma = 1.0$ ,  $B_{\text{data}}$  drops by a factor of 2.9 and  $S_{MC}$  by a factor of 2.1 as  $p_{\min}$  is raised from 5.0 to  $20 \text{ GeV}/c$ .

The two muon candidates must be identified by separate counters. This requirement halves the background and only reduces dimuon efficiency by 11% for a uniformly populated Dalitz plot.

The  $D^+ \rightarrow \pi^+ \mu^+ \mu^-$  search must account correctly for feedthrough from misidentified  $D^+ \rightarrow \pi^- \pi^+ \pi^+$  and  $D_s^+ \rightarrow \pi^- \pi^+ \pi^+$  decays [10] (Fig. 2). First, the invariant mass spectrum, under a  $\pi^+ \mu^+ \mu^-$  hypothesis but with no muon ID requirement [Fig. 2(a)], is fit by the sum of an exponentially falling distribution and two Gaussians describing the  $D^+ \rightarrow \pi^- \pi^+ \pi^+$  and  $D_s^+ \rightarrow \pi^- \pi^+ \pi^+$  peaks (solid curve). Because of incorrectly assigned daughter masses, these  $\pi^- \pi^+ \pi^+$  signals are broadened and shifted downward by about  $15 \text{ MeV}/c^2$  from true parent masses. Central values and widths of these peaks are used in the fit described below. Next, the muon ID requirement is imposed, giving the spectrum shown by

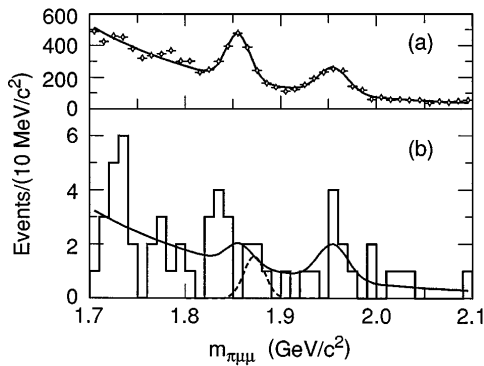


FIG. 2. Search for a  $D^+ \rightarrow \pi^+ \mu^+ \mu^-$  signal. (a) Invariant mass spectrum under a  $\pi^+ \mu^+ \mu^-$  hypothesis but with no muon identification requirement (diamonds). The curve, which is a fit by the sum of Gaussian peaks from misidentified  $D^+ \rightarrow \pi^- \pi^+ \pi^+$  and  $D_s^+ \rightarrow \pi^- \pi^+ \pi^+$  and an exponential background, determines the central values and widths of the peaks. (b) Invariant  $\pi^+ \mu^+ \mu^-$  mass spectrum for events with muon identification (histogram). The solid curve is the best fit to a sum of contributions from  $D^+ \rightarrow \pi^+ \mu^+ \mu^-$ , feedthrough from  $D^+ \rightarrow \pi^- \pi^+ \pi^+$  and  $D_s^+ \rightarrow \pi^- \pi^+ \pi^+$ , and an exponential background. The dashed curve shows the size and shape of the  $D^+ \rightarrow \pi^+ \mu^+ \mu^-$  contribution ruled out at 90% C.L.

the histogram in Fig. 2(b). We then search for a FCNC signal using a binned maximum likelihood fit with four components: a Gaussian centered at the  $D^+$  mass for  $D^+ \rightarrow \pi^+ \mu^+ \mu^-$ , two Gaussians describing feedthrough from  $D^+ \rightarrow \pi^- \pi^+ \pi^+$  and  $D_s^+ \rightarrow \pi^- \pi^+ \pi^+$ , and an exponential distribution. The central values and widths of the feedthrough peaks are constrained to the values from the fit in Fig. 2(a), and the width of the signal Gaussian is fixed at its observed value in  $D^+ \rightarrow \pi^- \pi^+ \pi^+$  decays, 11 MeV/ $c^2$ . The sizes of the four contributions are allowed to vary independently. The result of this fit is shown by the solid curve in Fig. 2(b). We find  $0.35^{+3.04}_{-2.47}$  events from  $D^+ \rightarrow \pi^+ \mu^+ \mu^-$ . The 90% confidence level (C.L.) upper limit is 4.36 events, determined by the point at which the log-likelihood function falls below its maximum value by  $(1.28)^2/2$ . The size and shape of the signal excluded at 90% C.L. is shown by the dashed curve.

Variations on this technique give consistent results. Specifying widths of the expected FCNC signal between 11 and 15 MeV/ $c^2$  changes the upper limit by only 4%. Constraining the relative amounts of  $D^+ \rightarrow \pi^- \pi^+ \pi^+$  and  $D_s^+ \rightarrow \pi^- \pi^+ \pi^+$  feedthrough to be the same as in Fig. 2(a) gives  $<3.2$  events at 90% C.L., while use of a simple mass window instead of a likelihood fit gives  $<4.5$  events. We have also tested the procedure with ensembles of simulated experiments in which fixed numbers (2–10) of simulated FCNC signal events, drawn randomly from a Gaussian mass distribution, are added to the observed spectrum and successfully found by the fit.

The 90% C.L. upper limit on the branching fraction  $B$  for  $D^+ \rightarrow \pi^+ \mu^+ \mu^-$  is given by

$$B(D^+ \rightarrow \pi^+ \mu^+ \mu^-) < \frac{U(\pi^+ \mu^+ \mu^-)}{N(K^- \pi^+ \pi^+)} \frac{1}{\eta_\mu} f_{\text{sys}} B_N,$$

where  $U(\pi^+ \mu^+ \mu^-) = 4.36$  is the 90% C.L. upper limit on the number of signal events,  $N(K^- \pi^+ \pi^+) = 37006 \pm 204$  is the number of events in the normalizing channel,  $\eta_\mu = 0.625 \pm 0.075$  is the relative efficiency of the  $\pi^+ \mu^+ \mu^-$  and  $K^- \pi^+ \pi^+$  channels,  $f_{\text{sys}} = 1.03$  is the factor [11] by which the limit is degraded by systematic uncertainties, and  $B_N = B(D^+ \rightarrow K^- \pi^+ \pi^+) = (9.1 \pm 0.6)\%$  [12].

The relative efficiency  $\eta_\mu$  is determined primarily from a Monte Carlo calculation. It includes factors arising from different decay kinematics ( $1.12 \pm 0.10$ ), the 7 GeV/ $c$  muon track momentum requirement ( $0.96 \pm 0.01$ ), muon ID ( $0.67 \pm 0.03$ ) and separate-counter ( $0.89 \pm 0.03$ ) requirements, and relative trigger efficiency ( $0.98 \pm 0.03$ ). The systematic uncertainties which give rise to  $f_{\text{sys}}$ , totaling 15% when added in quadrature, include those in  $N(K^- \pi^+ \pi^+)$ ,  $\eta_\mu$ , and  $B(D^+ \rightarrow K^- \pi^+ \pi^+)$ . The factor  $f_{\text{sys}}$  is calculated from the prescription of Ref. [11].

At 90% C.L.,  $B(D^+ \rightarrow \pi^+ \mu^+ \mu^-) < 1.8 \times 10^{-5}$ . The limit is quite stable under variation of vertex selection and muon ID criteria. Expressed as a measurement, the result is  $B(D^+ \rightarrow \pi^+ \mu^+ \mu^-) = (0.14^{+1.2}_{-1.0}) \times 10^{-5}$ , where quoted errors are statistical only; systematic errors, approximately 15% of  $B$ , are negligible by comparison.

Monte Carlo calculations show that the experimental acceptance is nearly uniform across the  $\pi^+ \mu^+ \mu^-$  Dalitz plot for squared dimuon mass  $m_{\mu\mu}^2$  greater than 0.8 (GeV/ $c^2$ )<sup>2</sup>. For smaller  $m_{\mu\mu}^2$  the acceptance decreases roughly linearly to near zero at minimum  $m_{\mu\mu}^2$  [13].

The search for  $D^+ \rightarrow \pi^+ e^+ e^-$  employs vertex selection and  $D^+ \rightarrow K^- \pi^+ \pi^+$  exclusion criteria identical to those for  $\pi^+ \mu^+ \mu^-$ . Candidate  $D^+ \rightarrow \pi^+ e^+ e^-$  decays contain two oppositely charged tracks identified as electrons and have  $\pi^+ e^+ e^-$  invariant mass consistent with  $D^+$ .

Electron ID is based on energy deposition and transverse shower shape, and position in the calorimeter. Calorimeter response was studied with topologically identified  $e^+ e^-$  pairs from  $\gamma$  conversions upstream of the tracking, and with pions from kinematically identified  $K_s^0 \rightarrow \pi^+ \pi^-$  decays. Electron ID efficiency and hadron mis-ID probability were measured as a function of particle momentum  $p$  for varying shower criteria. For the FCNC limit, a mis-ID probability of 0.8% was chosen by again optimizing  $S_{\text{MC}}/\sqrt{B_{\text{data}}}$ . Electron efficiency then varies from 62% to 45% for  $9 < p < 20$  GeV/ $c$ .

A search-window procedure (Fig. 3) is used for  $D^+ \rightarrow \pi^+ e^+ e^-$ . One of the three candidates is inside the window 1.830 to 1.890 GeV/ $c^2$ , which was chosen from a simulated signal. The  $\pi^+ e^+ e^-$  spectrum without electron ID is normalized to two events outside the search window, and then used to predict the expected number inside the window,  $0.42 \pm 0.29$  event, giving a signal

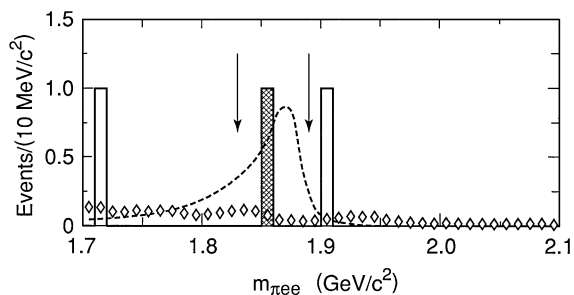


FIG. 3. Search for a  $D^+ \rightarrow \pi^+ e^+ e^-$  signal: invariant mass spectrum with a  $\pi^+ e^+ e^-$  hypothesis. Three events pass electron identification requirements (histogram). One of them is in the signal region between the arrows. Background is estimated from the  $\pi^+ e^+ e^-$  invariant mass spectrum without electron identification requirement, normalized to two events outside the signal region (diamond points). The dashed curve shows the size and shape of the bremsstrahlung-widened  $D^+ \rightarrow \pi^+ e^+ e^-$  signal excluded at 90% C.L.

of  $0.58 \pm 1.04$  event. A standard method for Poisson processes with background [12] gives 3.56 events as the 90% C.L. upper limit for one signal and 0.42 expected background events. The size and shape of the signal excluded at 90% C.L. is shown by the dashed curve.

The  $B(D^+ \rightarrow \pi^+ e^+ e^-)$  upper limit is obtained from

$$B(D^+ \rightarrow \pi^+ e^+ e^-) < \frac{U(\pi^+ e^+ e^-)}{N(K^- \pi^+ \pi^+)} \frac{1}{\eta_e} f_{\text{sys}} B_N,$$

where  $U(\pi^+ e^+ e^-) = 3.56$  events at 90% C.L.,  $N(K^- \pi^+ \pi^+) = 37006 \pm 204$  events in the normalizing channel,  $\eta_e = 0.138 \pm 0.021$ , and  $f_{\text{sys}} = 1.04$ . The relative efficiency  $\eta_e$  of  $\pi^+ e^+ e^-$  and  $K^- \pi^+ \pi^+$ , determined from a Monte Carlo calculation, is dominated by the dielectron detection efficiency ( $0.32 \pm 0.02$ ) and by the exclusion of much of the expected long bremsstrahlung tail in a  $D^+ \rightarrow \pi^+ e^+ e^-$  mass peak from the mass window ( $0.66 \pm 0.08$ ). The systematic uncertainties which give rise to  $f_{\text{sys}}$  [11], totaling 16% when added in quadrature, include those in  $N(K^- \pi^+ \pi^+)$ ,  $\eta_e$ , and  $B(D^+ \rightarrow K^- \pi^+ \pi^+)$ .

At 90% C.L.,  $B(D^+ \rightarrow \pi^+ e^+ e^-) < 6.6 \times 10^{-5}$ . The branching fraction with one-standard-deviation errors is  $B(D^+ \rightarrow \pi^+ e^+ e^-) = (1.0 \pm 1.9) \times 10^{-5}$ . Efficiency across the Dalitz plot is fairly uniform for squared dielectron masses  $m_{ee}^2$  above about  $0.4$  ( $\text{GeV}/c^2$ )<sup>2</sup>, but decreases roughly linearly to near zero at minimum  $m_{ee}$  [13].

In summary, Fermilab experiment E791 has obtained upper limits on branching fractions  $B$  for the three-body FCNC decays  $D^+ \rightarrow \pi^+ \mu^+ \mu^-$  and  $D^+ \rightarrow \pi^+ e^+ e^-$  that are an order of magnitude below those previously published. At 90% C.L.,  $B(D^+ \rightarrow \pi^+ \mu^+ \mu^-) < 1.8 \times 10^{-5}$  and  $B(D^+ \rightarrow \pi^+ e^+ e^-) < 6.6 \times 10^{-5}$ .

These limits can constrain extensions to the standard model [3]. For example, if a new neutral gauge boson  $X$  couples the  $c$  and  $u$  quarks with strength similar to those of allowed weak couplings, one expects  $B(D^+ \rightarrow$

$\pi^+ l^+ l^-) \tau_{D^0}/B(D^0 \rightarrow \pi^- l^+ \nu) \tau_{D^+} \approx m_W^4/m_X^4$ . Inserting our upper limit for  $B(D^+ \rightarrow \pi^+ \mu^+ \mu^-)$  and known values [12] of  $B(D^0 \rightarrow \pi^- e^+ \nu) = 3.9 \times 10^{-3}$  and the lifetime ratio  $\tau_{D^0}/\tau_{D^+} = 0.39$  into this expression gives the constraint  $m_X \gtrsim 390 \text{ GeV}/c^2$ .

We thank the staffs of Fermilab and all participating institutions for their assistance. This research was supported by the Brazilian Conselho Nacional de Desenvolvimento Científico e Tecnológico, CONACyT (Mexico), the Israeli Academy of Sciences and Humanities, the Fulbright Foundation, the U.S. Department of Energy, the U.S.-Israel Binational Science Foundation, and the U.S. National Science Foundation. Fermilab is operated by the Universities Research Association, Inc., under contract with the U.S. Department of Energy.

- [1] S. L. Glashow, J. Iliopoulos, and L. Maiani, Phys. Rev. D **2**, 1285 (1970).
- [2] All references to  $D^+$  and  $D_s^+$  and their decay modes imply also the corresponding charge-conjugate states.
- [3] See, e.g., K. S. Babu *et al.*, Phys. Lett. B **205**, 540 (1988); A. S. Joshipura, Phys. Rev. D **39**, 878 (1989).
- [4] A. J. Schwartz, Mod. Phys. Lett. A **8**, 967 (1993).
- [5] CLEO Collaboration, P. Haas *et al.*, Phys. Rev. Lett. **60**, 1614 (1988); Mark II Collaboration, A. J. Weir *et al.*, Phys. Rev. D **41**, 1384 (1990).
- [6] E653 Collaboration, K. Kodama *et al.*, Phys. Lett. B **345**, 85 (1995).
- [7] J. A. Appel, Annu. Rev. Nucl. Part. Sci. **42**, 367 (1992), and references therein; D. J. Summers *et al.*, Proceedings of the XXVII Rencontre de Moriond, Electroweak Interactions and Unified Theories, Les Arcs 1992 (unpublished), p. 417; S. Amato *et al.*, Nucl. Instrum. Methods Phys. Res., Sect. A **324**, 535 (1993).
- [8] V. K. Bharadwaj *et al.*, Nucl. Instrum. Methods **155**, 411 (1978); V. K. Bharadwaj *et al.*, Nucl. Instrum. Methods Phys. Res., Sect. A **228**, 283 (1985); D. J. Summers, Nucl. Instrum. Methods Phys. Res., Sect. A **228**, 290 (1985).
- [9] Outer edges of the calorimeter have strips 6.34 cm wide.
- [10] Feedthrough from misidentified  $D^+ \rightarrow K^- \pi^+ \pi^+$  is well separated from  $D^+ \rightarrow \pi^+ \mu^+ \mu^-$ , but rises steeply for  $\pi^+ \mu^+ \mu^-$  mass below  $1.80 \text{ GeV}/c^2$ . To avoid adding fit parameters to describe this rise, we exclude  $K^- \pi^+ \pi^-$  masses between  $1.850$  and  $1.890 \text{ GeV}/c^2$ .
- [11] R. D. Cousins and V. L. Highland, Nucl. Instrum. Methods Phys. Res., Sect. A **320**, 331 (1992).
- [12] Particle Data Group, L. Montanet *et al.*, Phys. Rev. D **50**, 1203 (1994).
- [13] The reader can use this approximate dependence of E791 acceptance on  $m_{\ell\ell}^2$  to estimate sensitivity with various matrix elements  $|M|$ . For example, if  $|M|^2 \sim (1 - m_{\ell\ell}^2/M_D^2)^2$  as in a  $V$ -type decay, the quoted acceptance gives 17% (9%) lower E791 sensitivity for  $\pi^+ \mu^+ \mu^-$  ( $\pi^+ e^+ e^-$ ) with this  $|M|^2$  than with the phase-space distribution assumed in our limits. For hypothesized  $|M|^2$  peaking sharply at low  $m_{\ell\ell}$  [e.g., G. Burdman (private communication)], E791 sensitivity is considerably reduced.